Volume 8, Issue 4, 2018, 3400 - 3404 ISSN 2069-5837

Biointerface Research in Applied Chemistry

www.BiointerfaceResearch.com

Original Research Article Open Access Journal

Received: 16.07.2018 / Revised: 08.08.2018 / Accepted: 12.08.2018 / Published on-line: 15.08.2018

Zinc aluminate nano-powders efficient promoter for the removal of indigo carmine from synthetic wastewaters

Sadaf Janghorban [1], Majid Ghashang [1, *]

[1]Department of Chemistry, Faculty of Sciences, Najafabad Branch, Islamic Azad University, Najafabad, Iran; P.O. Box: 517, Tel: +98-3142291004; Fax: +98-3142291016;

*corresponding author e-mail address: ***ghashangmajid@gmail.com***

ABSTRACT

A simple procedure for the removal of inserted dyes into the aquatic environment has been developed for the adsorption of indigo carmine from synthetic wastewater onto zinc aluminate ($ZnAl_2O_4$) nano-powder. $ZnAl_2O_4$ was prepared *via* a co-precipitation method and characterized by XRD, FE-SEM, and TEM techniques. The results of investigations show the good efficiency of $ZnAl_2O_4$ nano-powder as an adsorbent for the adsorption of indigo carmine dye. The effect of various parameters including pH, contact time, dye concentration, and absorbent dosage have been investigated.

Keywords: *$ZnAl_2O_4$ nano-powders; Indigo carmine; dye removal, absorption.*

1. INTRODUCTION

During the years, a significant amount of pigments such as indigo-carmine are wasted and eaten into the environment as wastewater during dying and dyeing processes. The addition of colored sewage to water resources, in addition to undesirable appearance, reduces the water use utilization in urban, agricultural and industrial uses and causes the environment to be inappropriate for recreational purposes such as swimming, fishing, and tourism [1]. Water coloration prevents photosynthesis activities due to reduced light penetration in water. Also, the presence of aromatic compounds in some dyes causes carcinogenicity and toxicity. Therefore, these dyes are placed in the category of hazardous environmental pollutants. So far dye removal has been studied using different methods [1]. In the meantime, physical methods such as direct deposition (flocculation), separation (ultrafiltration and oscillation) and activated carbon adsorption do not result in the removal and degradation of the pollutant molecule and only transfer it from one environment to another. Biological methods, due to the toxicity and toughness of the degradability of the aromatic compounds, have not been efficiently used. The absorption process is such an easy and cheap removal way of dyes from wastewaters [2]. Historically, different adsorbents have been used, e.g., zeolite, metal oxide and carbon active. Amongst of different adsorbents, metal oxides are widely used due to the flexibility and ease of preparation, as well as high efficiency to remove toxic dyes such as methylene blue, malachite green and so-on [2].

Indigo, a natural organic pigment with an attractive blue color, is derived from the *Indigofera tinctoria* plant and has been considered in the textile industry as one of the most relevant colorants. Indigo carmine with the ionic structure is given in Scheme 1, has usages in food and cosmetics industrial fields, as well as a microscopic stain in biology [3].

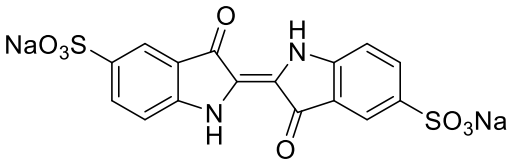

Scheme 1 Structure of indigo carmine blue dye.

The adsorption treatment is a useful technique for the removal of indigo carmine dye from wastewater. Mesoporous Mg/Fe layered double hydroxide [4], bottom ash and de-oiled soya [5], Mg-Al–CO_3-calcined layered double hydroxides [6], rice husk ash [7], nano Al-MCF [8], and activated carbon [9], are some of the adsorbents used for the efficiently removal of indigo carmine.

In continue of our investigation on the nano-catalysis, we reported here the efficient removal of indigo carmine dye *via* $ZnAl_2O_4$ nano-powders [10-22].

2. EXPERIMENTAL SECTION

Anhydrous $ZnCl_2$, $Al(NO_3)_3.9H_2O$, and other chemicals were purchased from Merck/Aldrich companies. X-Ray diffraction (XRD) patterns were measured on a Bruker diffractometer (D_8-Advance, axes) using Cu-Kα irradiation. FE-SEM images were taken on a Hitachi S-4160 photograph instrument. TEM micrographs were observed *via* an HU-12A electron microscope (Hitachi, Japan).

2.1. Preparation of $ZnAl_2O_4$. Two a solution of zinc chloride (10 mmol) and aluminum nitrate (20 mmol) in 125 mL of water, amino-ethanol (120 mmol dissolved in 250 ml H_2O) was added dropwise under vigorous magnetic stirring. The precipitate is left for 30 minutes; then it is filtered and dried. The resulting compound is calcined at a temperature of 750 ° C for 3 hours.

2.2. Adsorption experiments. Five solutions of indigo carmine dye with an initial concentration of 10, 20, 40, 60, and 80 ppm

were prepared each of them is 100 mL in volume. The initial pH of the solutions was adjusted to the required value (4,6, 8, 9, 10) by adding either HCl (1M) or NaOH (1M) solution. The experiments were performed on a 20 mL container. The volume of each sample was 10 mL. The catalysts were added to the specimens and then stirred at ambient temperature for 80 minutes. For analysis, the specimens were first kept at rest while the catalyst was precipitated and then analyzed using high-performance liquid chromatography (HPLC). Different parameters such as dye concentration, pH, and catalyst dosages were investigated.

The bellow equation calculated the adsorption percentage:

$$\%A = \frac{C_0 - C_t}{C_0} * 100 \qquad (1)$$

Where A is a yield of the adsorption, C_0 and C_t are the concentrations of dye at time 0 and t, respectively.

The quantity of retained indigo carmine (q_e), was calculated according to the following equation: $q_e = (C_i - C_e)V/m$ while C_i and C_e are initial and equilibrium concentrations of indigo carmine, m is the mass of the $ZnAl_2O_4$, and V is the volume of the solution [10-12].

3. RESULTS SECTION

Zinc aluminate was prepared in natural atmosphere and investigated using X-ray diffraction (XRD), FE-SEM, and TEM.

In order to fission and to determine the crystalline grain size of the synthesized product, X-ray diffraction (XRD) test was performed. The XRD pattern state that the zinc aluminate crystallized in the cubic phase with characteristic peaks of 36.6, 43.0, 52.6, 55.8, 57.8, 65.6, 70.5, and 77.4 [2θ °] (Figures 1).

The mean crystallite size of nanoparticles was measured as 63 nm by the Scherrer equation:

$$A = 0.9\lambda/\beta\cos\theta$$

The parameters A, λ, and β are defined as average crystallite size, X-ray wavelength (1.54 Å), and full-width at half-maximum (FWHM) of the intensity peak in radian, and θ is the Bragg angle.

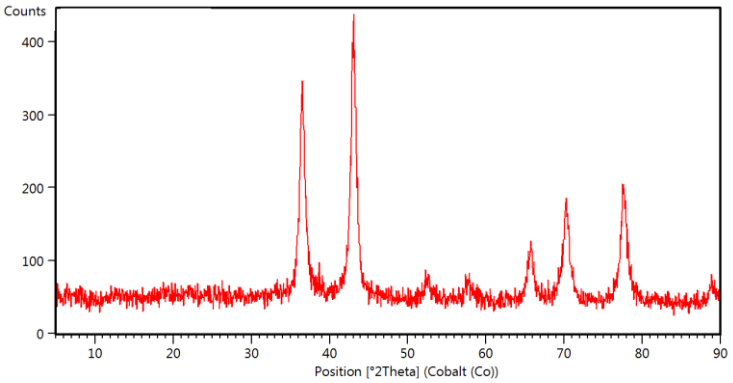

Fig. 1. XRD pattern of $ZnAl_2O_4$ nano-powders.

The surface morphology was investigated by FE-SEM and TEM analysis (Figure 2). From FE-SEM images, it was revealed that the powder is made up of often spherical particles. TEM image provides evidence that the nanoparticles are in diameter of less than 100 nm without severe agglomeration.

3.1. Adsorption measurements.

3.1.1. Effect of contact time. The effect of contact time on the absorption of indigo carmine dye on $ZnAl_2O_4$ nano-powders has a deep insight into the removal mechanism. The adsorption experiments as a function of time were investigated under the ambient temperature at the constant condition of indigo carmine concentration 40 ppm, $ZnAl_2O_4$ nano-powders dosage as catalyst 0.05 g, pH=9 (Figure 3). The results show that the maximum absorption of dye (86%) occurs in the first 50 minutes, and after that, it will be almost negligible and remained constant up to 80 min. It is revealed that surface area is controlling the rate of the adsorption and the short adsorption time is due to the high surface area of $ZnAl_2O_4$ nano-powders which attract a rapidly large number of dye molecules.

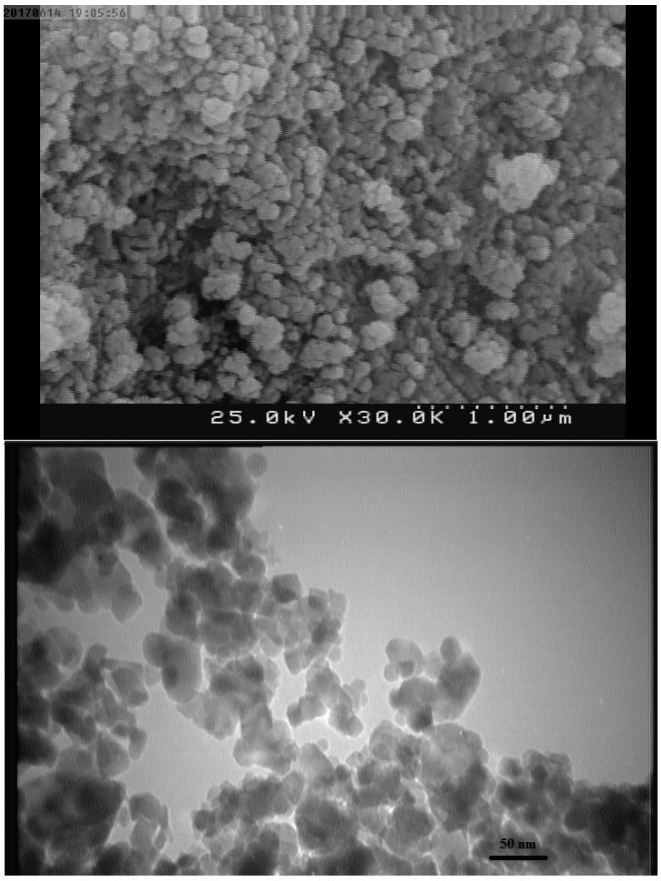

Fig. 2. FE-SEM and TEM analysis of $ZnAl_2O_4$ nano-powders.

3.1.2. The pH Effect. The surface charge of both indigo carmine dye and $ZnAl_2O_4$ nano-powders could be influenced by the pH of the solution when adsorption proceeds. Thus the interaction between indigo carmine dye and $ZnAl_2O_4$ nano-powders which depends on the functional groups will be changed at the acidic and basic condition. The adsorption results at different pH are summarized in Figure 4. The experiments were done at dye concentration as 40 ppm, $ZnAl_2O_4$ nano-powders dosage as 0.05

g, and time as 80min. Figure 4 shows a maximum of absorption of 86% at pH=9. Below and higher values of pH have a lower percentage of adsorption dye and its removal from water media. In pH=10, dye adsorption yield is reduced because the hydroxyl ions and the pigment anions are involved in a competition to be adsorbed on the surface of $ZnAl_2O_4$ nano-powders. In natural and acidic media, the electrostatic charges are similar which causes to the lower adsorption capacity [10-12].

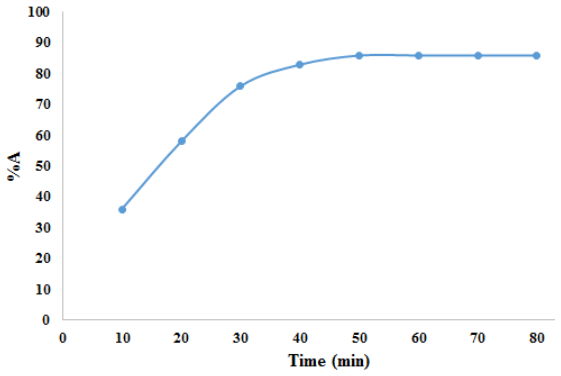

Fig. 3. Effect of contact time on the absorption of indigo carmine dye on $ZnAl_2O_4$ nano-powders

3.1.3. Effect of dye concentration. Next, the effect of the initial concentration of indigo carmine dye was investigated (Figure 5). The adsorption experiments were carried out under ambient temperature when pH was adjusted as 9, $ZnAl_2O_4$ nano-powders dosage as 0.05 g and adsorption proceeded time as 80min. The adsorption is in higher of its value as 40 ppm (86%) of dye concentration and is lower at 50 (71%), 30 (84%), 20 (79%), and 10 ppm (71%) values. Due to the surface saturation, adsorption is reduced with the increasing of dye concentration from 40 ppm value [13].

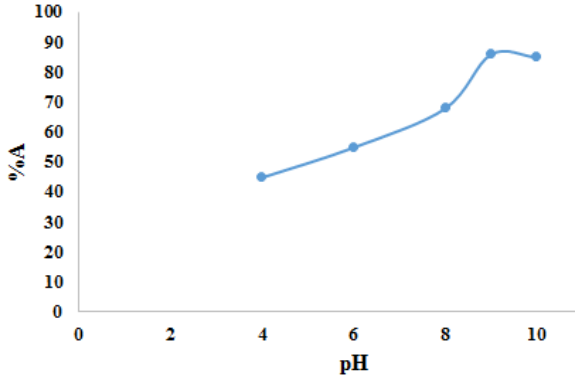

Fig. 4. Effect of pH on the absorption of indigo carmine dye on $ZnAl_2O_4$ nano-powders.

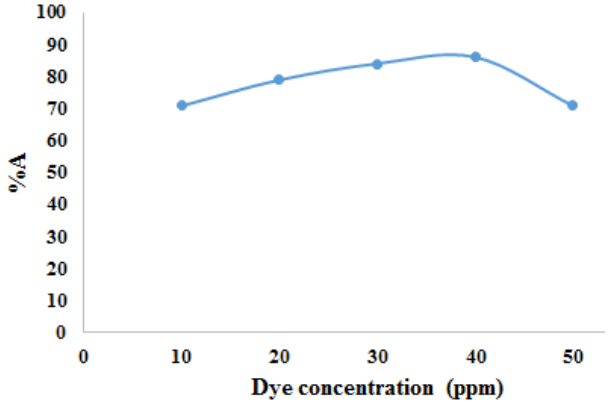

Fig. 5. Effect of dye concentration on the absorption of indigo carmine dye on $ZnAl_2O_4$ nano-powders.

3.1.4. Effect of catalyst dosages. The optimum amount of catalyst required for the adsorption of the maximum amount of indigo carmine was examined by varying the catalyst dosages from 0.01 to 0.1 g (Figure 6). The maximum amount of adsorption (86%) is achieved when 0.05 g of $ZnAl_2O_4$ nano-powders was used while pH=9, and dye concentration (40 ppm) are constant. By increasing the dosages of nanomaterial, the adsorption efficiency of dye was increased so that in 0.05 g of catalyst dosage the adsorption was reached to their higher values. In Higher values of catalyst dosages adsorption is reduced because catalyst particles agglomerated and their surface area is reduced [10-13].

3.2. Adsorption isotherm models.

Adsorption isotherms were used, to provide a clear indication of the distribution of color molecules in two phases at the equilibrium condition and homogeneity of the adsorbent surface. In this, Freundlich and Langmuir adsorption models were used under the constant condition of $ZnAl_2O_4$ nano-powders dosage 0.05 g, and pH=9 as well as indigo carmine concentrations including 10, 20, 30, 40, 50 ppm, (Figure 7). The constants and coefficients of the Freundlich and Langmuir models are summarized in Table 1. Based on the correlation coefficient (R^2), the Langmuir model has the better fitness in the adsorption process. This shows that the adsorption of indigo carmine takes place on the surface of $ZnAl_2O_4$ nano-powders. Moreover, the Langmuir constants and coefficients (Table 1) indicating that the monolayer adsorption of indigo carmine is favorable (R^2 = 0.95) under the operating conditions.

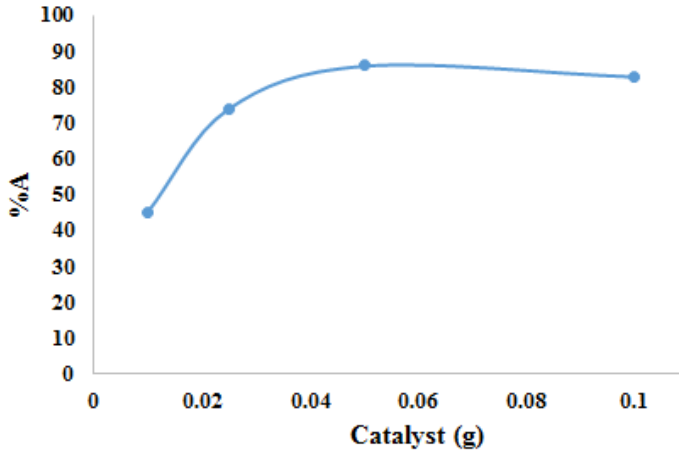

Fig. 6. Effect of catalyst dosage on the absorption of indigo carmine dye on $ZnAl_2O_4$ nano-powders.

Table 1. Langmuir and Freundlich Parameters and correlation coefficient (R^2) constants.

Isotherm	Equation	Parameters	R^2
Langmuir	$\frac{1}{q_e} = \frac{1}{q_m K_L C_e} + \frac{1}{q_m}$	K_l= -0.124; q_m = -2.68	0.95
Freundlich	$\log(q_e) = \log(K_f) + \frac{1}{n}\log(C_e)$	n = 1.14; K_f = 0.91	0.61

C_e (mg L^{-1}) is the equilibrium concentration; q_e (mg g^{-1}) is the uptake of the indigo carmine; q_m (mg g^{-1}) is the maximum adsorption capacity of nano-powders; K_L (L mg^{-1}) is the Langmuir adsorption equilibrium constant; K_F (L/mg) and n are the Freundlich constants

Table 2. The related parameters of kinetic models and correlation coefficient (R^2) constants.

Model	Equation	Parameters	R^2
pseudo-first-order	$\ln (q_e-q_t) = \ln (q_e) - k_1 t$	K_1= 0.09	0.978
pseudo-second-order	$\frac{t}{q_t} = \frac{1}{k_2 q_e^2} + \frac{t}{q_e}$	k_2 = 0.012	0.98
Intra-particle diffusion	$q_t = k_i (t)^{0.5} + c$	c = 1.69; k_i = 0.66	0.81

q_t (mg g^{-1}) is the adsorption capacity at time t, q_e (mg g^{-1}) the adsorption capacity at equilibrium, k_1, and k_2 rate constants (min^{-1}), t is the contact time (min), k_i (mg g^{-1} $min^{-1/2}$) is the intra-particle diffusion rate constant, and c (mg g^{-1}) is a constant proportional to the thickness of the boundary layer

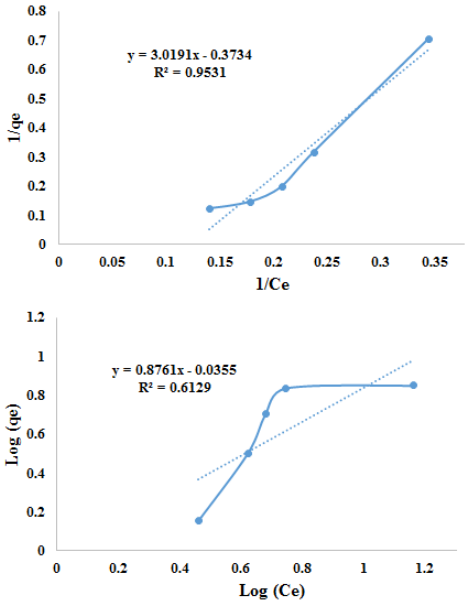

Fig. 7. Freundlich and Langmuir adsorption models.

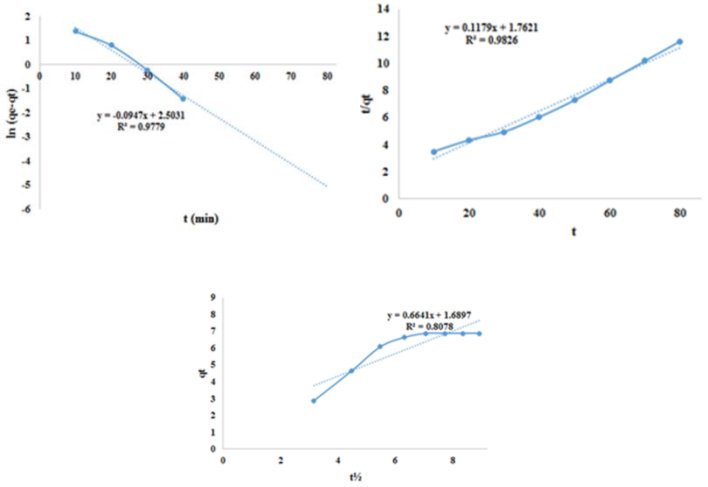

Fig. 8. Kinetic models of dye adsorption: from bottom intramolecular diffusion, pseudo-second order, and pseudo-first order models

3.3. Kinetics of adsorption.

In adsorption studies, the kinetic investigation will be of a useful way to predict the rate of the adsorption onto $ZnAl_2O_4$ nano-powders for understanding the mechanism of the adsorption process. Three models including pseudo-first order, pseudo-second order, and intramolecular diffusion are applied to investigate the kinetics of dye adsorption (Figure 8). The equations and related parameters are shown in Table 2.

The linear relationship of $\ln(q_e- q_t)$ versus t, t/q_t versus t and q_t versus $t^{0.5}$ is used to evaluate the k_1, k_2 and k_i values in the investigated models (Figure 8) [10-12]. The pseudo-first-order model applies only at pre-equilibrium times and thus is inapplicable to describe the kinetics of dye adsorption. The higher correlation coefficient (R^2) of the pseudo-second-order model indicates the applicability of this model to explain the kinetics of the adsorption.

4. CONCLUSIONS

In conclusion, we think that the procedure for the preparation of $ZnAl_2O_4$ nano-powders is so simple and could be applied for the preparation of other nanostructures. $ZnAl_2O_4$ nano-powders were found to be an effective catalyst and adsorbent for the removal of indigo carmine dye from synthetic wastewater. The obtained results show that the best condition for the achievement of the maximum adsorption is catalyst dosage (0.05 g), pH=9, and dye concentration (40 ppm). Our studies show that the Langmuir isotherm theory could explain the adsorption mechanism. The results of the kinetics showed that the dye absorption was fitted pseudo-second-order kinetic model according to its higher correlation coefficient.

5. REFERENCES

[1] Lichtfouse E., Schwarzbauer J., Robert D., *Environmental Chemistry: Green Chemistry and Pollutants in Ecosystems*. Springer Science & Business Media, **2005**.
[2] Gupta V.K., Suhas, Application of low-cost adsorbents for dye removal – A review. *Journal of Environmental Management*, 90, 2313–2342, **2009**.
[3] Sabnis R.W., *Handbook of Biological Dyes and Stains: Synthesis and Industrial Applications*. John Wiley & Sons, New Jersy, **2010**.
[4] Ahmed M.A., brick A.A., Mohamed A.A., An efficient adsorption of indigo carmine dye from aqueous solution on mesoporous Mg/Fe layered double hydroxide nanoparticles prepared by controlled sol-gel route. *Chemosphere*, 174 280-288, **2017**.
[5] Mittal A., Mittal J., Kurup L., Batch and bulk removal of hazardous dye, indigo carmine from wastewater through adsorption. *Journal of Hazardous Materials B*, 137, 591–602, **2006**.
[6] El Gaini L., Lakraimi M., Sebbar E., Meghea A., Bakasse M., Removal of indigo carmine dye from water to Mg–Al–CO3-calcined layered double hydroxides. *Journal of Hazardous Materials*, 161, 627–632, **2009**.
[7] Arenas C.N., Vasco A., Betancur M., Martínez J.D., Removal of

Indigo Carmine (IC) from aqueous solution by adsorption through abrasive spherical materials made of rice husk ash (RHA). *Process Safety and Environmental Protection*, 106, 224-238, **2017**.
[8] Hashemian S., Sadeghi B., Mangeli M., Hydrothermal synthesis of nano cavities of Al-MCF for adsorption of indigo carmine from aqueous solution. *Journal of Industrial and Engineering Chemistry*, 21, 423-427, **2015**.
[9] Hu Y., Chen X., Liu Z., Wang G., Liao S., Activated carbon doped with biogenic manganese oxides for the removal of indigo carmine. *Journal of Environmental Management*, 166, 512-518, **2016**.
[10] Zare M., Ghashang M., Saffar-Teluri A., BaO-ZnO nano-composite efficient catalyst for the photo-catalytic degradation of 4-chlorophenol. *Biointerface Research in Applied Chemistry*, 6, 1049-1052, **2016**.
[11] Khosravian P., Ghashang M., Ghayoor H., Zinc oxide/natural-Zeolite composite nano-powders: Efficient catalyst for the amoxicillin removal from wastewater. *Biointerface Research in Applied Chemistry*, 6, 1538-1540, **2016**.
[12] Khosravian P., Ghashang M., Ghayoor H., Effective removal of penicillin from aqueous solution using Zinc oxide/natural-Zeolite composite nano-powders prepared via ball milling technique. *Recent Patents on Nanotechnology*, 11, 154-164, **2017**.
[13] Azadeh M., Mousavi S., Ghashang M., Photocatalytic degradation of phenol in aqueous media over $BaAl_2O_4$-SrO composite nanofibers. *Biointerface Research in Applied Chemistry*, 7, 2166 – 2169, **2017**.
[14] Ghashang M., $ZnAl_2O_4$–Bi_2O_3 composite nano-powder as an efficient catalyst for the multi-component, one-pot, aqueous media preparation of novel 4H-chromene-3-carbonitriles. *Research on Chemical Intermediates*, 42, 4191-4205, **2016**.
[15] Nazemi A., Mohammad Shafiee M.R., Ghashang M., ZnO-CaO-MgO nanocomposite: efficient catalyst for the preparation of thieno[2,3-d]pyrimidin-4(3H)-one derivatives. *Biointerface Research in Applied Chemistry*, 7, 2135 -2139, **2017**.
[16] Ghashang M., Mansoor S.S., Mohammad Shafiee M.R., Kargar M., Biregan M.N., Azimi F., Taghrir H., Green chemistry preparation of MgO nanopowders: efficient catalyst for the synthesis of thiochromeno[4, 3-b]pyran and thiopyrano[4, 3-b]pyran derivatives. *Journal of Sulfur Chemistry*, 37, 377-390, **2016**.
[17] Baziar A., Ghashang M., Preparation of pyrano [3, 2-c] chromene-3-carbonitriles using ZnO nano-particles: a comparison between the Box–Behnken experimental design and traditional optimization methods. *Reaction Kinetics, Mechanisms and Catalysis*, 118, 463–479, **2016**.
[18] Ghashang M., Mansoor S.S., Solaree L.S., Sharifian-esfahani A., Multi-component, one-pot, aqueous media preparation of dihydropyrano [3,2-c]chromene derivatives over MgO nanoplates as an efficient catalyst. *Iranian Journal of Catalysis*, 6, 237-243, **2016**.
[19] Sheikhan-Shamsabadi N., Ghashang M., Nano-basic silica as an efficient catalyst for the multi-component preparation of pyrano [2, 3-d] pyrimidine derivatives. *Main Group Metal Chemistry*, 40, 19-25, **2017**.
[20] Ghashang M., An Aurivillius perovskite nano-structure of $SrBi_4Ti_4O_{15}$: efficient catalyst for the preparation of novel dihydronaphtho[2′,1′: 4,5]thieno[2,3-d]pyrimidin-7(6H)-one derivatives using HSBM technique. *Journal of the Iranian Chemical Society*, 15, 55-60, **2018**.
[21] Abbasi-Dehnavi H., Ghashang M., Solvent-free preparation of 3-aryl-2-[(aryl)(arylamino)] methyl-4H-furo[3, 2-c]chromen-4-one derivatives using ZnO-$ZnAl_2O_4$ nanocomposite as a heterogeneous catalyst. *Heterocyclic Communications*, 24, 19-22, **2018**.
[22] Ghashang M., Bi2O3 nano-particles as an efficient catalyst for the multi-component, one-pot, aqueous media preparation of benzo [h] pyrano [3, 2-c] chromene-2-carbonitriles and pyrano [3, 2-g] chromene-7-carbonitriles. *Biointerface Research in Applied Chemistry*, 6, 1338-1344, **2016**.

6. ACKNOWLEDGEMENTS

We are thankful to the Najafabad Branch, Islamic Azad University research council for partial support of this research